Plant Physiology Preview. Published on June 10, 2016, as DOI:10.1104/pp.16.00525

Short Title: A Pseudophosphatase Controls Dormancy Variation

Corresponding Author:
Wim Soppe,
Department of Plant Breeding and Genetics, Max Planck Institute for Plant Breeding Research,
Carl-von-Linné-Weg 10, 50829 Cologne, Germany
Email: soppe@mpipz.mpg.de
Phone: 00492215062470

Title:
Sequence Polymorphisms at the Reduced Dormancy 5 Pseudophosphatase Underlie Natural Variation in Arabidopsis Dormancy

Yong Xiang[a,b], Baoxing Song[a], Guillaume Née[a,1], Katharina Kramer[c], Iris Finkemeier[c,1,], Wim J.J. Soppe[a,d,2]

[a]Department of Plant Breeding and Genetics, Max Planck Institute for Plant Breeding Research, Carl-von-Linné-Weg 10, 50829 Cologne, Germany
[b]Agricultural Genome Institute at Shenzhen, Chinese Academy of Agricultural Sciences, 518120 Shenzhen, China
[c]Plant Proteomics, Max Planck Institute for Plant Breeding Research, Carl-von-Linné-Weg 10, 50829 Cologne, Germany
[d]Institute of Molecular Physiology and Biotechnology of Plants (IMBIO), University of Bonn, 53115 Bonn, Germany

One sentence summary:
DELAY OF GERMINATION 18 QTL encodes a pseudophosphatase, involved in seed dormancy regulation.

Author Contributions:
Y.X., I.F. and W.J.J.S. designed the research. Y.X., B.S., G.N., and K.K. performed research. Y.X., B.S., G.N., and K.K. analyzed data. Y.X. and W.J.J.S. wrote the article.

Funding for this work is from Max-Planck Society.

[1] Current address: Institute of Plant Biology and Biotechnology, Schlossplatz 7, 48149 Münster, Germany
[2] Corresponding author: Wim Soppe, soppe@mpipz.mpg.de

ABSTRACT

Seed dormancy controls the timing of germination, which regulates the adaptation of plants to their environment and influences agricultural production. The time of germination is under strong natural selection and shows variation within species due to local adaptation. The identification of genes underlying dormancy quantitative trait loci (QTL) is a major scientific challenge, which is relevant for agricultural and ecological goals. In this study, we describe the identification of the *DELAY OF GERMINATION 18* (*DOG18*) QTL, which was identified as a factor in natural variation for seed dormancy in *Arabidopsis thaliana*. *DOG18* encodes a member of the clade A of the type 2C protein phosphatases family, which we previously identified as the *REDUCED DORMANCY 5* (*RDO5*) gene. *DOG18*/*RDO5* shows a relatively high frequency of loss-of-function alleles in natural accessions restricted to northwestern Europe. The loss of dormancy in these loss-of-function alleles can be compensated by genetic factors like *DOG1* and *DOG6*, and by environmental factors such as low temperature. RDO5 does not have detectable phosphatase activity. Analysis of the phosphoproteome in dry and imbibed seeds revealed a general decrease in protein phosphorylation during seed imbibition that is enhanced in the *rdo5* mutant. We conclude that RDO5 acts as a pseudophosphatase that inhibits dephosphorylation during seed imbibition.

INTRODUCTION

Survival of plants depends on their control of seed germination timing because this indirectly determines the conditions during all subsequent phases of the life cycle. Seed dormancy prevents germination under (temporary) favorable conditions and can delay seedling establishment until the onset of the growth season. This makes it an important factor in the adaptation of plants to their local environment. The level of seed dormancy is influenced by environmental conditions experienced by the mother plant and by the seeds during storage in the seed bank, in particular temperature, humidity, light, and nitrate. In *Arabidopsis thaliana* (Arabidopsis), low temperatures experienced by the mother plant during seed maturation are known to enhance seed dormancy. In contrast, low temperatures during seed imbibition promote germination (Footitt et al., 2011; Kendall et al., 2011; Graeber et al., 2012; He et al., 2014). Changes in dormancy are coupled with an altered balance between the levels of the plant hormones abscisic acid (ABA) and gibberellin (GA), which are also reflected by the transcript levels of genes controlling hormone synthesis and breakdown. ABA is required for the induction of dormancy, whereas GA is necessary for germination. The biosynthesis and signalling pathways of both hormones negatively influence each other (Nambara et al., 2010; Graeber et al., 2012). Members belonging to clade A of the type 2C protein phosphatases (PP2Cs) have important roles in ABA-dependent dormancy by inhibiting the activity of SNF1-related kinases (SnRKs) via dephosphorylation (Park et al., 2009).

Arabidopsis grows in large areas of the northern hemisphere and is adapted to different environments. This is reflected in seed dormancy variation between accessions and its underlying genetic variation (Springthorpe and Penfield, 2015). Therefore, it is not surprising that analyses of natural variation in seed dormancy between Arabidopsis accessions yielded several dormancy QTLs (Alonso-Blanco et al., 2003; Bentsink et al., 2010). A major QTL, *DELAY OF*

79 *GERMINATION 1* (*DOG1*), was identified in the progeny of a cross between the low dormant
80 accession Landsberg *erecta* (L*er*) and the highly dormant accession Cape Verde Islands (Cvi).
81 *DOG1* has been cloned and turned out to be a conserved key regulator of seed dormancy (Bentsink
82 et al., 2006). The amount of DOG1 protein in freshly harvested seeds showed a strong positive
83 correlation with dormancy levels. Interestingly, DOG1 transcript and protein levels are increased
84 by low temperatures during seed maturation, corresponding with enhanced dormancy levels
85 (Kendall et al., 2011; Nakabayashi et al., 2012).
86 Here, we report the cloning and analysis of a gene underlying the seed dormancy QTL *DOG18*,
87 which was identified in crosses of L*er* with three other accessions (Bentsink et al., 2010). *DOG18*
88 encodes a family member of the PP2C phosphatases named REDUCED DORMANCY 5 (RDO5).
89 We had previously identified this gene based on the low dormancy level of its mutant (Xiang et al.,
90 2014). We now show that RDO5 functions as a pseudophosphatase that influences the seed
91 phosphoproteome. *DOG18* has extensive sequence variation among accessions and a high
92 frequency of potential loss-of-function alleles with a geographic distribution limited to
93 northwestern Europe. The influence of *DOG18* on seed dormancy can be modified by other
94 dormancy QTLs like *DOG1* and *DOG6*, and by the temperature experienced by the mother plant
95 during seed maturation.
96
97

RESULTS

Fine-Mapping of *DOG18*

The seed dormancy QTL *DOG18* has been identified in recombinant inbred line (RIL) populations derived from crosses between L*er* and the accessions Antwerpen-1 (An-1), Santa Maria da Feira-0 (Fei-0), and Kashmir-2 (Kas-2) (Bentsink et al., 2010). *DOG18* is a relatively weak QTL in comparison with *DOG1* and its L*er* allele enhances dormancy in all three populations. *DOG18* has been located in a 2 cM region on chromosome 4 (Supplemental Figure 1A; Bentsink et al., 2010). The Near-Isogenic Line DOG18-Fei-0 (NIL DOG18) contains an introgression of Fei-0 encompassing the *DOG18* QTL in the L*er* background and shows reduced seed dormancy compared to L*er* (Figure 1A). Fine mapping of *DOG18* using progeny from a cross between NIL DOG18 and L*er* narrowed down its location to a 700 Kb region (Supplemental Figure 1B). A recently cloned dormancy gene, *RDO5*, is located in this region making it a strong candidate for the gene underlying the QTL (Xiang et al., 2014). A comparison of the *RDO5* genomic sequence between the four accessions showed that An-1 and Fei-0 contain an identical one bp deletion in the second exon, leading to a frame shift and early STOP codon. The Kas-2 allele of *RDO5* still encodes a full-length protein, but has four amino acid changes in comparison to the L*er* allele (Figure 1B and Supplemental Figure 1C). Recently, the same gene was also identified to underlie the germination QTL *IBO*, which was detected in a cross between the accessions Eilenburg-0 (Eil-0) and Loch Ness-0 (Lc-0). The Lc-0 allele enhances dormancy and has a, thus far unique, single bp change causing an A to E substitution in a highly conserved PP2C motif (Amiguet-Vercher et al., 2015).

To obtain additional evidence that *RDO5* is the gene underlying *DOG18*, complementation experiments were carried out. We transformed NIL DOG18 with a construct containing the *RDO5*

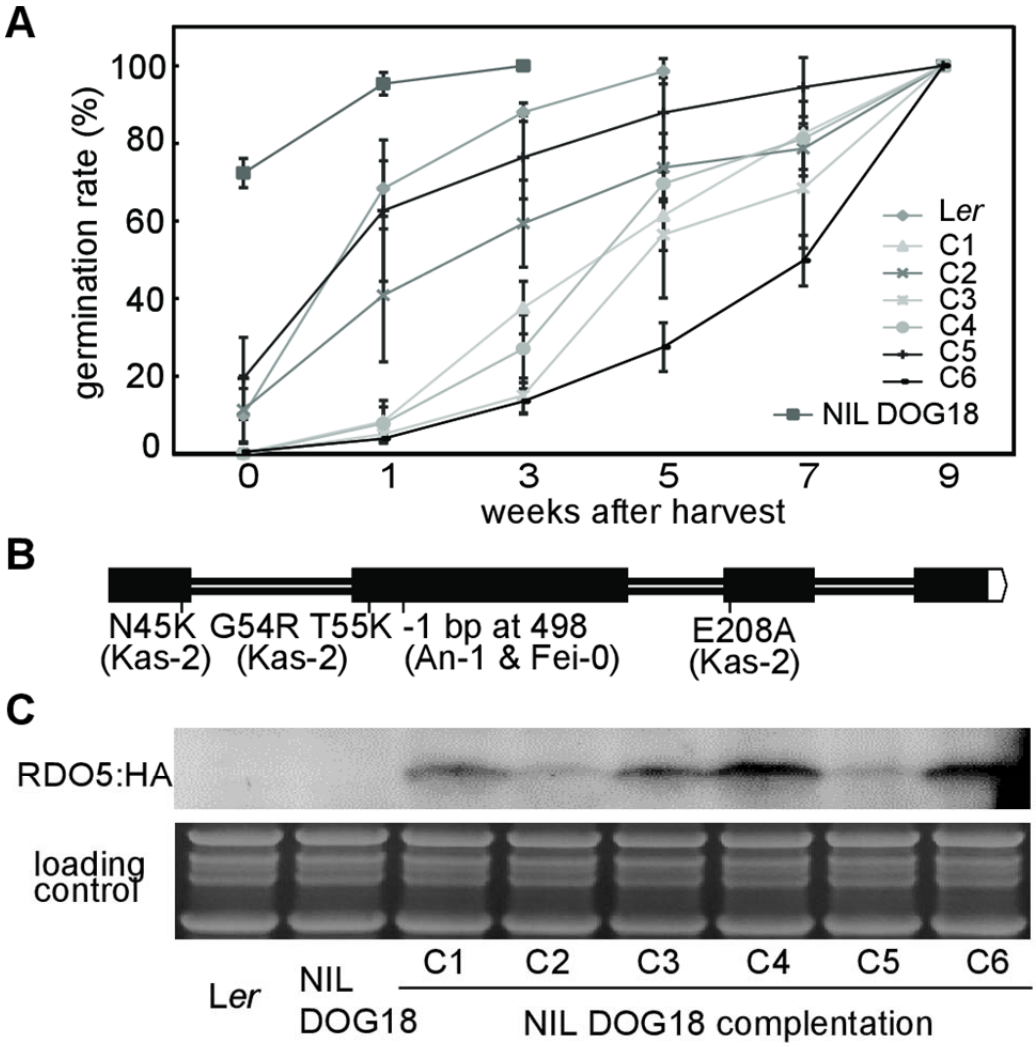

Figure 1. Complementation of DOG18 by *RDO5*.
(A) Germination after different periods of dry storage of seeds from L*er*, NIL DOG18 and six independent transgenic NIL DOG18 lines containing the *RDO5* gene from L*er*. Shown are means ± SE of six to eight independent batches of seeds for each genotype.
(B) Gene structure of *RDO5* and natural polymorphisms identified in the An-1, Fei-0 and Kas-2 accessions compared to L*er*. Exons are shown as black boxes and introns as lines.
(C) Immunoblot analysis of RDO5:HA protein accumulation in seeds of the six NIL DOG18 complementation trangenic lines from (A). Coomassie Brilliant Blue (CBB) staining was used as a loading control.

promoter and gene from L*er*, fused with a C-terminal HA tag. Six independent transformants with a single introgression event were selected. All of these showed enhanced dormancy compared to NIL DOG18 (Figure 1A). Moreover, the amount of RDO5:HA protein in the transformants

correlated with their seed dormancy level confirming previous observations (Xiang et al., 2014). Lines 2 and 5 showed dormancy levels similar to the L*er* accession and contained less RDO5:HA protein in their seeds than the other four transformants. Line 6 with a high RDO5:HA abundance showed a high dormancy level (Figure 1A, C). Additionally, the Fei-0 allele of *RDO5* was introduced into the *rdo5-1* mutant, which has very low dormancy levels (Xiang et al., 2014). Three independent homozygous single insertion transformants all showed a complete lack of complementation, indicating that the *RDO5* Fei-0 allele is not functional (Supplemental Figure 1D).

Loss-of-function *RDO5* Alleles are Frequently Found in Northwestern European Accessions

We were interested to find out whether the *RDO5* Fei-0/An-1 specific allele is more widespread among Arabidopsis accessions. Therefore, a dCAPs marker was designed for this one bp deletion. A population of about 360 diverse accessions from the haplotype map collections (Li et al., 2010) was screened and the deletion was found in two additional accessions, Cam61 and Lac-3 (Supplemental Figure 2). Fei-0 and Lac-3 are moderately dormant, but An-1 and Cam61 have low dormancy levels. We investigated whether the seed dormancy level of An-1 and Cam61 could be enhanced by introducing a genomic fragment containing the functional *RDO5* allele from L*er* driven by its native promoter. Three independent homozygous single insertion transformants with enhanced *RDO5* transcript levels in seeds were obtained for both accessions (Supplemental Figure 3A-B). All transformants showed increased dormancy levels compared to the wild-type An-1 and Cam61 accessions (Figure 2A-B). We have previously shown that the reduced dormancy phenotype of the *rdo5* mutant requires enhanced transcript levels of the *Arabidopsis PUMILIO 9* (*APUM9*) gene, which encodes a protein belonging to the conserved PUF family of RNA binding

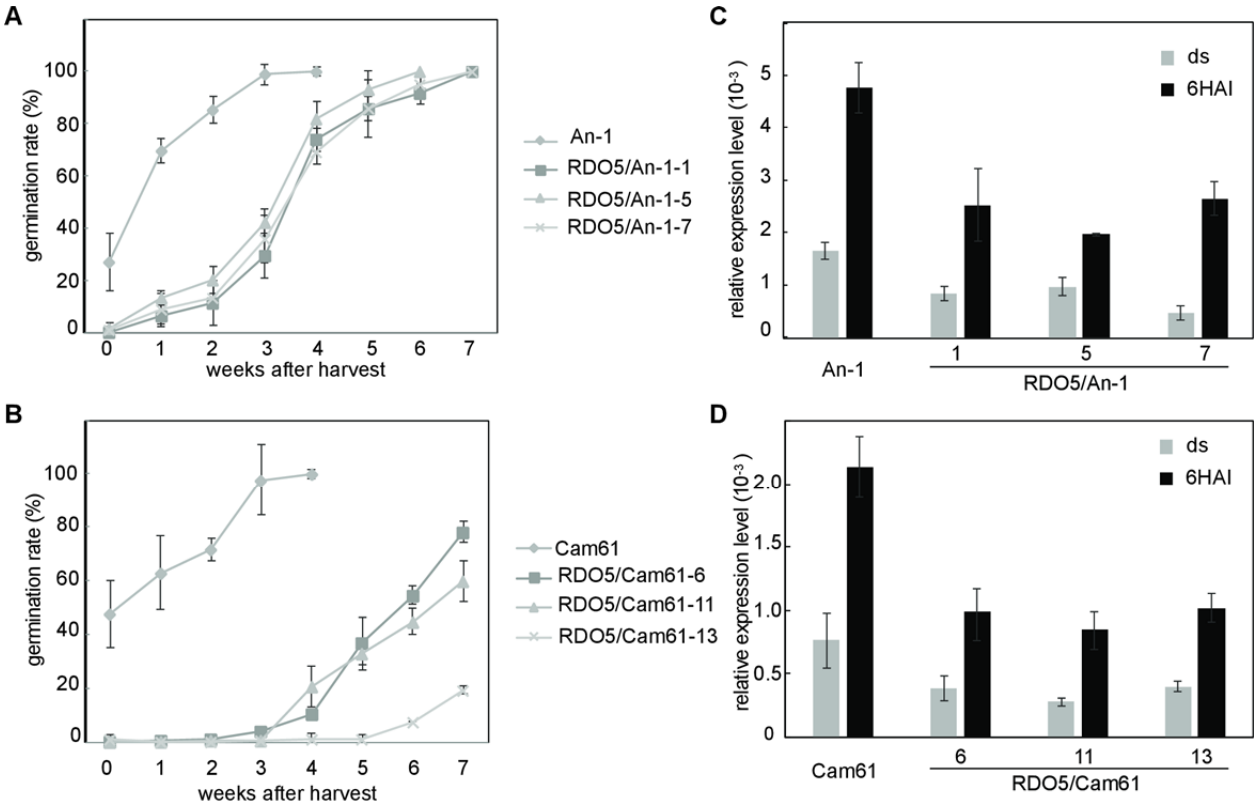

Figure 2. Complementation of An-1 and Cam61 by *RDO5*.
(A) and (B), Germination after different periods of dry storage of seeds from transgenic lines containing the *RDO5* L*er* allele in An-1 (A) or Cam61 (B) background. Shown are averages ± SE of six to eight independent batches of seeds for each genotype.
(C) and (D) qRT-PCR analysis of *APUM9* transcript levels in dry and 6HAI seeds in An-1 (C), Cam61 (D) and their transgenic lines. The expression values were normalized using *ACT8* as control. n = 3 biological replicates; error bars represent SE.

proteins (Xiang et al., 2014). Interestingly, introduction of the wild-type L*er RDO5* gene in the An-1 and Cam61 accessions caused a significant decrease in *APUM9* transcript levels in both dry seeds and those imbibed for six hours (6HAI) (Figure 2C-D). This suggests that a reduction in *APUM9* transcript levels by introduction of a functional *RDO5* gene contributes to the enhanced dormancy levels in these two accessions.

To identify additional alleles of *RDO5*, we analyzed sequences from nearly 870 accessions of the 1001 genome project with a world-wide distribution (http://1001genomes.org). Forty-two of these accessions contained *RDO5* alleles that were predicted to have lost their function because of a single bp change leading to a STOP codon in the second exon, small deletions causing frame shifts and early STOP codons, large deletions, or a splice site mutation causing a frame shift (Figure 3

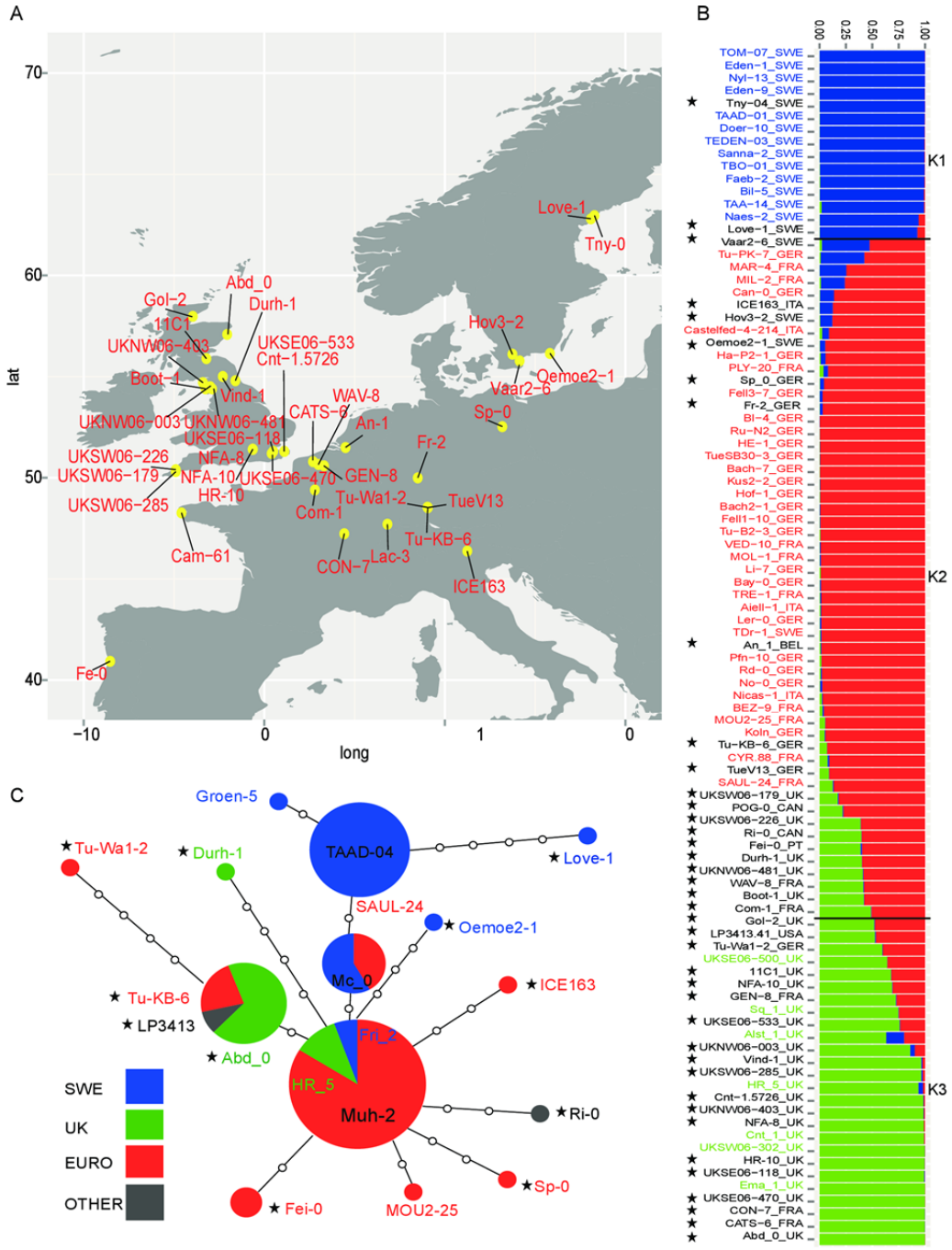

Figure 4. Geographic distribution, population structure and haplotype network of accessions containing *RDO5* loss-of-function alleles.
(A) Geographical distribution of 42 accessions harboring *RDO5* predicted loss-of-function alleles.
(B) Population structure of 95 accessions containing functional or predicted loss-of-function *RDO5* alleles originating from Sweden, UK and Western Europe at K=3. Black stars indicate accessions carrying *RDO5* loss-of-function alleles.
(C) *RDO5* haplotype network. Haplotypes are represented by circles with sizes proportional to the number of populations containing that haplotype. Each node represents a single mutation. Black stars indicate accessions or groups carrying *RDO5* loss-of-function alleles.

and Supplemental Table 1). Most of the accessions with nonsense mutations and indels are predicted to encode truncated proteins with a similar length as the protein encoded by the Fei-0 allele, for which we showed that it has lost its ability to induce dormancy (Supplemental Figure

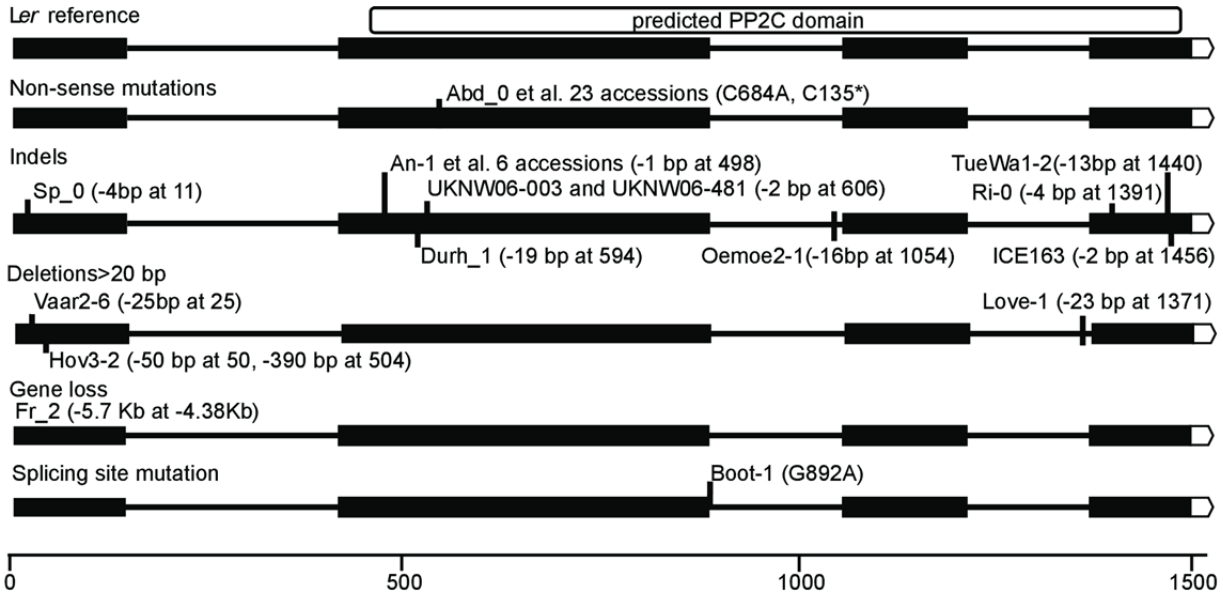

Figure 3. Natural loss-of-function mutations in the *DOG18* gene.
Natural mutations causing predicted *DOG18* loss-of-function alleles are divided into five groups that are shown in separate rows. The location of the mutations for the individual accessions are indicated. Exons (black boxes) are connected with horizontal lines representing intronic regions of *DOG18*. The location of the predicted PP2C domain is indicated at the top.

1D). Interestingly, nearly all of the 42 accessions were located in a relatively small region of Europe consisting of the United Kingdom, northern France and southwestern Germany, as well as in coastal regions of Sweden (Figure 4A). These regions have a mild oceanic climate with evenly dispersed rainfall and relatively small temperature changes during the year. Ri-0 and POG-0 originated from Canada and LP3413.41 originated from the USA. The accession Fei-0 originated from Portugal, but was collected in a very humid environment that is atypical for that region (personal communication, C. Alonso-Blanco). The genetic relationships among the potential loss-of-function *RDO5* accessions were determined using a structure analysis, which indicated that the loss-of-function alleles of *RDO5* had three different origins (Figure 4B) and can be divided in three main haplotypes representative for Sweden, Western Europe and the United Kingdom (Supplemental Figure 4). Accessions Ri-0 and POG-0 clustered with the haplotypes from Western Europe and LP3413.41 with the UK, suggesting that these accessions originated from these regions (Figure 4B). A haplotype network analysis of 132 different accessions, including the 32

predicted loss-of-function *RDO5* accessions revealed the existence of 14 independent haplotypes including one cluster of 22 identical alleles with a single bp change causing a STOP codon and a second cluster of 3 alleles with a 1bp deletion including Fei-0 and An-1 alleles. In addition, multiple independent deletions causing frame shifts occurred (Figure 4C). Therefore, independent *RDO5* loss-of-function alleles seem to have arisen from different parental alleles.

Factors Enhancing Seed Dormancy in Accessions Containing *RDO5* Loss-of-function Alleles

We analyzed seed dormancy in 11 accessions with potential *RDO5* loss-of-function alleles and found considerable variation. Several accessions showed high dormancy levels (Figure 5A), which was not expected considering the very low seed dormancy of the loss-of-function *rdo5-1* mutant (Xiang et al., 2014). In addition, we observed extensive variation in dormancy within F2 progenies of crosses between the *rdo5-2* mutant (in Col background) and the Fei-0 and Lac-3 accessions that contain *RDO5* loss-of-function alleles (Supplemental Figure 5). These observations indicated that a loss of *RDO5* can be compensated by other genetic factors. Besides *DOG18*, ten additional QTLs for seed dormancy have been found that could be candidates for these factors; among them, the two strongest are *DOG1* and *DOG6* (Bentsink et al., 2010).

To study the role of DOG1 on dormancy in the absence of functional RDO5, DOG1 protein levels were analyzed in a set of *RDO5* loss-of-function accessions with varying amounts of seed dormancy. In general, low dormant accessions showed a low abundance of DOG1 protein, whereas highly dormant accessions showed high levels of DOG1. A few exceptions, like Cam61 and Fr-2 showed relatively high DOG1 protein levels with low dormancy levels, whereas HR-10 showed relatively low DOG1 protein level and a high dormancy level (Figure 5B). A comparison of the *DOG1* alleles showed that two of the accessions (An-1 and Fr-2) contained the DSY

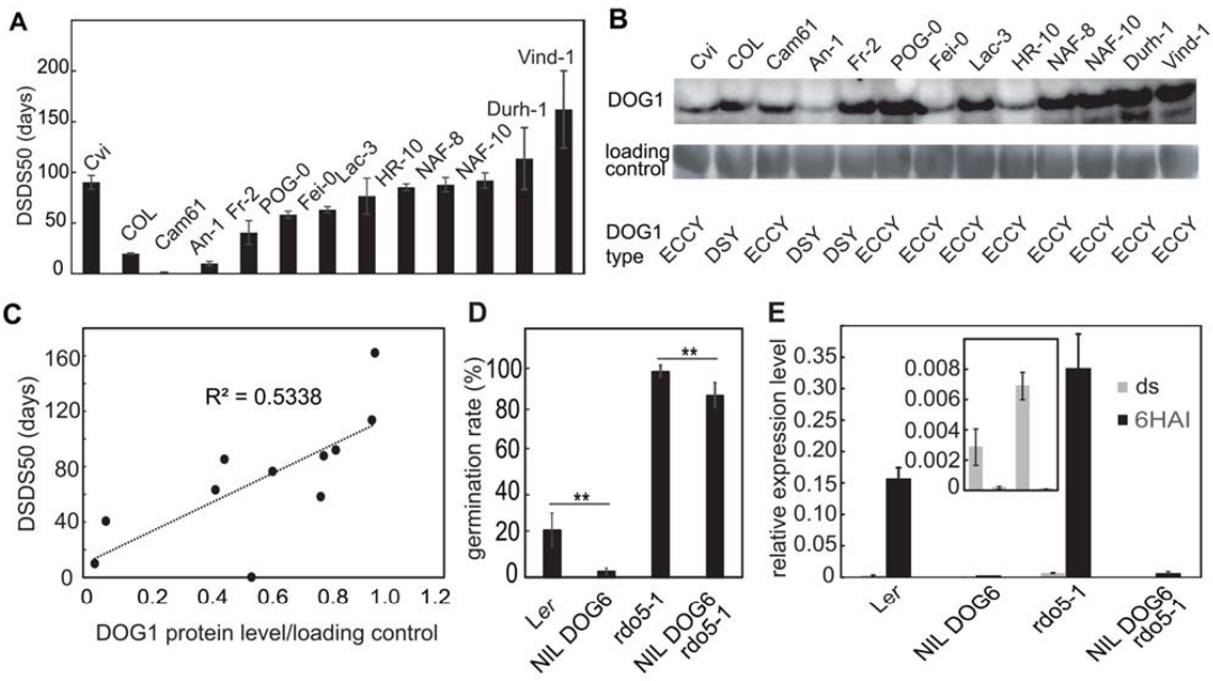

Figure 5. Genetic modifiers of the *RDO5* phenotype.
(A) Dormancy level of 11 accessions with predicted loss-of-function *RDO5* alleles. Col and Cvi are used as low and high dormancy controls. POG-0, HR-10, NFA-8, Vind-1 and NFA-10 belong to the non-sense mutation group, An-1, Fei-0, Lac-3, Cam61 and Durh-1 belong to the indels group, and Fr-2 belongs to the gene loss group. Shown are means ± SE of six to eight independent batches of seeds for each genotype. DSDS50, days of seed dry storage required to reach 50% germination.
(B) Immunoblot analysis of DOG1 protein accumulation using a DOG1 antibody in the 11 accessions with predicted loss-of-function *RDO5* alleles. A band from the CBB staining was used as a loading control. The lower panel indicates the DOG1 haplotype of the accessions, ECCY is a strong allele and DSY is a weak allele.
(C) The correlation of dormancy level and DOG1 protein abundance (quantified from Figure 5B and normalized by the loading control).
(D) A strong *DOG6* allele from the Shahdara accession enhances dormancy of the *rdo5-1* mutant (in Ler background). Germination percentages were determined in freshly harvested seeds. Shown are means ± SE of six to eight independent batches of seeds for each genotype. **P < 0.01.
(E) qRT-PCR analysis of *APUM9* transcript levels in L*er*, *rdo5-1* (L*er* background), NIL DOG6 and *rdo5-1* NIL DOG6 dry and 6HAI seeds. Inset, *APUM9* expression in dry seeds from the different genotypes at a magnified scale. The expression values were normalized using *ACT8* as control. n = 3 biological replicates; error bars represent SE.

haplotype, which has a strongly reduced function compared to the ECCY *DOG1* haplotype that was present in the other 8 accessions (Nakabayashi et al., 2015) (Figure 5B). When we considered the functionality of the DSY *DOG1* allele to be 1/10 of that of the *ECCY* DOG1 allele, a positive correlation was found between DOG1 protein level and dormancy level (R^2=0.53, p=0.01) (Figure 5C). Therefore, high DOG1 protein accumulation is one possible way for seeds to hide the phenotypic effect of *RDO5* loss-of-function alleles.

The restriction of natural loss-of-function *RDO5* alleles to a relatively small region of

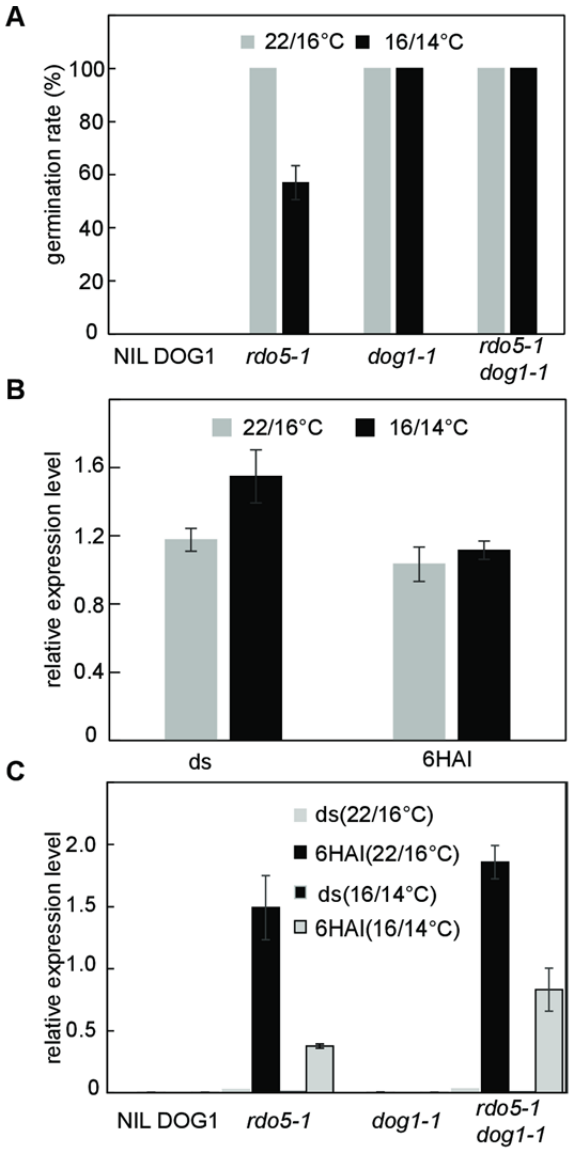

Figure 6. Maternal temperature affects the *RDO5* dormancy phenotype.
(A) Germination of NIL DOG1, *rdo5-1*, *dog1-1* and *rdo5-1 dog1-1* freshly harvested seeds that matured under a day/night regime of 22/16°C or 16/14°C. Shown are means ± SE of six to eight independent batches of seeds for each genotype.
(B) qRT-PCR analysis of *RDO5* transcript levels in NIL DOG1 dry and 6HAI seeds that matured under a day/night regime of 22/16°C or 16/14°C. The expression values were normalized using *ACT8* as control. n = 3 biological replicates; error bars represent SE.
(C) qRT-PCR analysis of *APUM9* transcript levels in NIL DOG1, *rdo5-1*, *dog1-1* and *rdo5-1 dog1-1* dry and 6HAI seeds that matured under a day/night regime of 22/16°C or 16/14°C. The expression values were normalized using *ACT8* as control. n = 3 biological replicates; error bars represent SE.

northwestern Europe could be related to temperature. We tested germination of the *rdo5-1* mutant and wild-type seeds maturing at higher (22/16°C) and lower (16/14°C) temperatures. The *rdo5-1* mutant completely lacked dormancy at higher temperatures, but showed increased dormancy at the

lower seed maturation temperature (Figure 6A). This might be caused by enhanced accumulation of DOG1 induced by low temperatures (Kendall et al., 2011; Nakabayashi et al., 2012). Indeed, the enhanced dormancy level of *rdo5-1* mutant seeds matured at low temperatures was lost in the *dog1-1* mutant background. This indicated that DOG1 is required to enhance seed dormancy at low temperatures in the *rdo5* mutant (Figure 6A). Interestingly, in contrast with *DOG1*, the transcript levels of *RDO5* were not affected by low temperatures (Figure 6B).

Because the RDO5 function is associated with decreased *APUM9* transcript levels (Xiang et al., 2014), we analyzed *APUM9* mRNA levels at both temperature regimes. As previously demonstrated (Xiang et al., 2014), *APUM9* expression level is highly increased in the *rdo5-1* background, especially in 6HAI seeds. The higher dormancy levels of seeds matured at lower temperatures was associated with reduced *APUM9* transcript levels (Figure 6C). However, the relation between reduced dormancy and enhanced *APUM9* transcription was not observed in the *dog1-1* mutant background, both in the presence and absence of *rdo5-1*. This suggests that *DOG1* influences dormancy independently of *APUM9*.

The relationship of *RDO5*/*DOG18* with *DOG6* was assessed by combining the *rdo5-1* mutant (in a L*er* background) with an introgression from the Shahdara accession containing a strong *DOG6* allele (Figure 5D). Analysis of germination of freshly harvested seeds showed that *DOG6* can enhance the dormancy level of *rdo5-1*, indicating an additive relation between *DOG6* and *RDO5*/*DOG18*. We also analyzed the *APUM9* transcript levels in the NIL DOG6 lines. Interestingly, we found that the enhancement in seed dormancy caused by the NIL DOG6 introgression was associated with strongly reduced *APUM9* transcript levels, both in the wild type and the *rdo5-1* mutant background (Figure 5E). This indicated that *APUM9* is not specific for the RDO5 pathway, but has a more general role in seed dormancy.

229

230 **RDO5 Functions as a Pseudophosphatase**

231 RDO5 is a member of the PP2C phosphatase family and enhances seed dormancy (Xiang et al.,
232 2014). Although RDO5 has strong homology with PP2Cs, it does not show complete sequence
233 conservation in amino acids essential for phosphatase activity. Amiguet-Vercher et al described
234 that in particular, RDO5 lacks conserved residues for metal coordination and phosphate binding
235 (Amiguet-Vercher et al., 2015). Interestingly, the D111 residue in RDO5 is a conserved G in active
236 PP2Cs. The replacement of this G to D in the clade A PP2C phosphatases HAB1, ABI1, ABI2 and
237 AHG3 caused loss of activity (Rodriguez et al., 1998; Gosti et al., 1999; Robert et al., 2006;
238 Yoshida et al., 2006). RDO5 also lacks about 40 amino acids in front of the MAPK docking site,
239 which is important for protein interaction (Supplemental Figure 6, 7 A-B). Gosti et al identified
240 five amino acid substitutions in this region in ABI1 that led to loss of activity indicating that this
241 domain is also important for activity (Gosti et al., 1999). In addition, RDO5 lacks a tryptophan
242 residue that is involved in the interaction with ABA in most ABA responsive PP2Cs. This may
243 explain why RDO5 does not affect ABA sensitivity (Xiang et al., 2014).
244 These observations suggest that RDO5 is not a catalytically active protein phosphatase. In
245 accordance, Amiguet-Vercher et al demonstrated very low phosphatase activity for RDO5 using *in*
246 *vitro* phosphatase assays (Amiguet-Vercher et al., 2015). We further confirmed these observations
247 and did not detect any phosphatase activity for RDO5 using the synthetic phospho-peptide
248 RRA(phosphoT)VA as substrate in the presence of either Mn^{2+} or Mg^{2+} as metal cofactor (Figure
249 7A). We were interested whether the phosphatase activity of RDO5 could be restored by
250 introducing back mutations to recover all the missing residues known to affect PP2C activity
251 (RDO5bm). Introduction of these back mutations into the RDO5 sequence indeed restored the

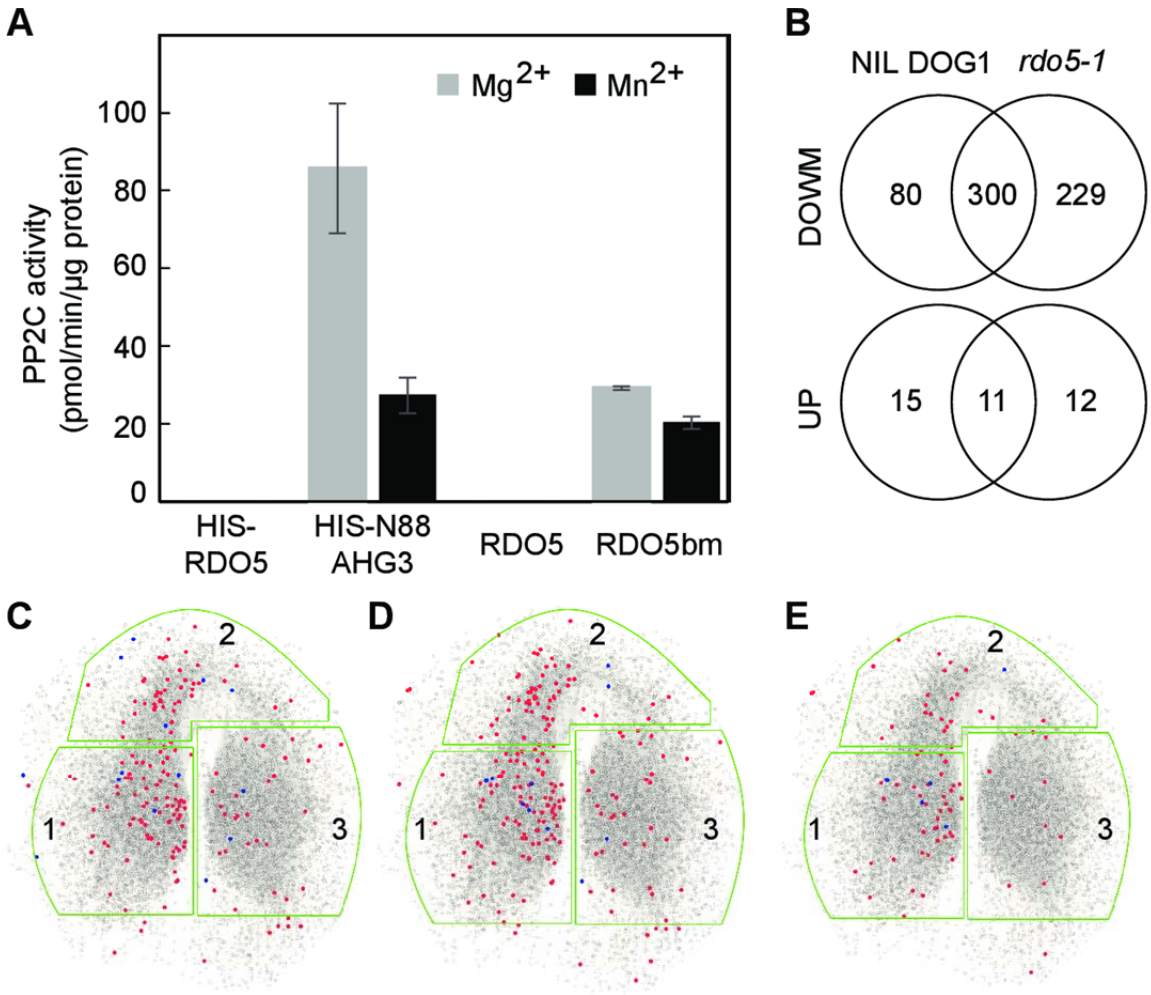

Figure 7. RDO5 functions as a pseudophosphatase.
(A) Phosphatase activity is restored in RDO5 after backmutations. Phosphatase activity of RDO5 and RDO5 back-mutation (RDO5bm) proteins was measured in vitro using the RRA(phosphoT)VA peptide as a substrate. ΔC-terN88AHG3 was used as a positive control. Data are averages ± SE from three replicates.
(B) Venn diagram analyses showing common and differential distribution of phosphorylated sites identified in NIL DOG1 and *rdo5-1* after six hours imbibition compared with dry seeds.
(C)-(E) Localization in the SeedNet network of differentially phosphorylated proteins from wild-type NIL DOG1 (C), *rdo5-1* (D) and differentially phosphorylated proteins present in *rdo5-1* but not in NIL DOG1 (E) after six hours imbibition compared with dry seeds. The regions outlined in green correspond to clusters associated with dormancy (region 1) or germination (regions 2 and 3). The red dots represent proteins with decreased phosphorylation levels and the blue dots represent proteins with increased phosphorylation levels.

phosphatase activity of RDO5 (Figure 7A, Supplemental Figure 6). RDO5bm displayed a specific activity of 29.1 $pmol.min^{-1}.mg^{-1}$ and 20.2 $pmol.min^{-1}.mg^{-1}$ with Mg^{2+} or Mn^{2+} as cofactors respectively. This activity is in a similar range as that of AHG3. These results suggest that RDO5

probably evolved from a functional PP2C phosphatase but has lost its phosphatase activity. Proteins homologous to phosphatases lacking essential amino acids for activity have previously been described as pseudophosphatases or anti-phosphatase proteins that might prevent specific residues from becoming dephosphorylated or phosphorylated by protecting them from real phosphatases or kinases (Reiterer et al., 2014). Thus we studied whether RDO5 could be a pseudophosphatase indirectly implied in the control of protein phosphorylation levels by comparing the phosphoproteome of the *rdo5-1* mutant with its wild-type NIL DOG1 in dry and 6 HAI seeds. A label-free quantitative mass spectrometry analysis on three biological replicates for each genotype and treatment identified 1527 phosphorylation sites in 875 protein groups. Imbibition of seeds caused a general decrease in phosphorylation, which was enhanced in the *rdo5* mutant (Figure 7B). In the wild-type NIL DOG1 background 380 phosphorylation sites in 238 proteins were significantly decreased after imbibition for 6 hours, whereas 26 phosphorylation sites in 20 proteins increased in phosphorylation status compared to dry seed. In the *rdo5-1* mutant 529 phosphorylation sites in 289 proteins were significantly decreased and 23 phosphorylation sites in 17 proteins increased in phosphorylation status compared with dry seed (Supplemental Table 2-3). In total, we found 229 phosphorylation sites with decreased phosphorylation levels and 12 phosphorylation sites with increased phosphorylation levels in *rdo5-1* compared to wild type (Figure 7B). These results indicated a general decrease in protein phosphorylation during seed imbibition that is enhanced in the *rdo5* mutant. We used SeedNet, a topological model of transcriptional interactions controlling dormancy and germination in Arabidopsis (Bassel et al., 2011), to study the relationship between the transcriptome and protein phosphorylation in imbibed seeds. The majority of differentially phosphorylated proteins after 6 HAI are located within region 1 that is associated with dormancy and in a section of region 2 that does not contain germination

associated genes. (Figure 7C-D) (Bassel et al., 2011). Proteins with altered phosphorylation levels specific in the *rdo5* mutant showed the same pattern (Figure 7E). These results suggest that the regulation of protein phosphorylation plays a role in the release of seed dormancy during early imbibition of seeds. Proteins directly involved in ABA signaling were not found among those with significant changes in phosphorylation level in *rdo5-1* seeds compared to the wild-type. This confirmed our previous observations that RDO5 is probably not part of the ABA pathway (Xiang et al., 2014).

RDO5 controls protein phosphorylation levels despite its lack of phosphatase activity. This control might occur by protecting proteins from dephosphorylation during imbibition because we identified more proteins with decreased phosphorylation levels in the *rdo5* mutant than in the wild type. Thus, our biochemical and proteomic results suggest that RDO5 acts as a pseudophosphatase.

In contrast to the changes observed in phosphoprotein abundance, from 5017 quantified protein groups only 106 (41 up-regulated and 65 down-regulated with a log2-fold change > 1) were significantly altered in abundance in wild type after 6h imbibition in comparison to dry seeds. In the *rdo5* mutant 132 proteins groups (48 up-regulated and 84 down-regulated with a log2-fold change > 1) were significantly altered upon imbibition (Supplemental Data set 1). Interestingly, only 29 of these regulated proteins overlapped between both genotypes. A SeedNet analysis showed that differentially expressed proteins are evenly located in the network (Supplemental Figure 8). Therefore, regulation of protein modifications seems to be more prominent during early seed imbibition compared to regulation of protein levels.

DISCUSSION

Seed dormancy has a high adaptive value for plants. Hence, it is not surprising that extensive natural variation exists for this trait. Exploring and identifying the underlying genes of this variation is important to understand plant adaptation and helpful to study the molecular mechanisms of dormancy. In Arabidopsis, several seed dormancy QTLs have been found. A major dormancy QTL locus, *DOG1*, was cloned nearly ten years ago and has been shown to be conserved within the plant kingdom (Ashikawa et al., 2010; Graeber et al., 2010). Here we report the identification of the underlying gene of a second dormancy QTL, *DOG18*. *DOG18* encodes a member of the type 2C protein phosphatase family that we previously identified as *RDO5*, which is a positive regulator of seed dormancy (Xiang et al., 2014). Natural variation at this gene has recently been described by the identification of a specific allele, IBO, which has a unique mutation in the Loch Ness accession, probably causing enhanced activity (Amiguet-Vercher et al., 2015).

We identified predicted loss-of-function *RDO5* alleles at a relatively high frequency in Arabidopsis accessions from northwestern Europe but could not detect any from other parts of the world (Figure 4A). Absence of RDO5 function could be an adaptation to the northwestern European climate of mild temperatures with low fluctuations and evenly dispersed rainfall. Interestingly, the non-dormant phenotype of the *rdo5-1* loss-of-function allele can be partially rescued when plants are grown at low temperatures. In addition, RDO5 enhances dormancy but is not essential for it, since accessions with loss-of-function *RDO5* alleles vary considerably in their dormancy levels (Figure 5A). This is consistent with the relatively weak effect on seed dormancy of the *DOG18* QTL compared with *DOG1* and *DOG6* (Bentsink et al., 2010). We assume that *RDO5* might have a neutral role or could even be under negative selection under specific environmental conditions prevalent in northwestern Europe. This could have led to the occurrence

of natural loss-of-function alleles that subsequently spread through the population. Interestingly, a QTL analysis of dormancy in two accessions from north-central Sweden and central Italy identified *DOG18* under greenhouse conditions but not in populations grown in the field. This is likely due to the lower temperatures in the field compared to the greenhouse, which mask the role of *DOG18* in dormancy (Postma and Agren, 2015).

We have identified two dormancy QTLs, *DOG1* and *DOG6*, that can partially rescue the *rdo5* mutant phenotype. Therefore, these QTLs contribute to explain differences in dormancy level between *RDO5* loss-of-function accessions. These results also confirm that different QTLs have additive roles in seed dormancy as previously suggested by Bentsink et al (Bentsink et al., 2010). Interestingly, in contrast to *DOG18*, naturally occurring loss-of-function alleles have never been identified for *DOG1*. This is consistent with the inability to induce seed dormancy in *dog1* mutant plants grown at low temperatures during seed maturation and the absence of loci that enhance dormancy in *dog1* loss-of-function alleles.

Despite its similarity to PP2C phosphatases, RDO5 is unlikely to be catalytically active as a phosphatase because it lacks several conserved residues. In accordance, we could not detect any phosphatase activity for RDO5. Amiguet-Vercher et al also reported a very low phosphatase activity for IBO/RDO5 (Amiguet-Vercher et al., 2015). It is likely that RDO5 has evolved from a functional phosphatase because we could recover its phosphatase activity by introducing amino acid changes to restore critical residues needed for activity (Figure 7 A, Supplemental Figure 6). These observations led us to propose that RDO5 could function as a pseudophosphatase. Pseudophosphatases have been described in humans and nematodes. For instance, human TAK-binding protein 1 (TAB1) is a member of the PPM family of protein phosphatases that does not show phosphatase activity. TAB1 possibly functions by binding to and controlling the

accessibility of phosphorylated residues on a kinase protein or its downstream substrates, thereby regulating pro-inflammatory signaling pathways (Conner et al., 2006). Pseudophosphatases, as well as pseudokinases, are increasingly seen as regulators of signaling pathways that can act as modulators, competitors or anchors of kinases and phosphatases (Reiterer et al., 2014).

Our comparison of the phosphoproteomes between wild-type NIL DOG1 and the *rdo5* mutant showed that RDO5 influences the phosphorylation status of hundreds of proteins, despite its lack of phosphatase activity. This is in agreement with its function as a pseudophosphatase. We suggest that RDO5 may bind to its target proteins to prevent them from dephosphorylation by other active protein phosphatases. Such a role for RDO5 would suggest an opposite function compared to other phosphatases. This hypothesis is supported by the positive role of RDO5 in seed dormancy (Xiang et al., 2014), which is contrasting with the negative roles of clade A PP2Cs like ABI1, ABI2, AHG1, and HAI2 (Rodriguez et al., 1998; Gosti et al., 1999; Nishimura et al., 2007; Kim et al., 2013). Amiguet-Vercher recently proposed a role for a unique natural allele of RDO5/IBO (from the Lc-0 accession) in ABA signaling because of its inhibitory influence on ABI phosphatase activity (Amiguet-Vercher et al., 2015). However, our phosphoproteome analysis did not give support for a general role of RDO5 in the ABA pathway because proteins involved in ABA signaling were not found among those with significant changes in phosphorylation level in *rdo5-1* mutant seeds. In addition, mutations in RDO5 neither affected ABA levels in dry and imbibed seeds nor ABA sensitivity during germination (Xiang et al., 2014). We observed a massive dephosphorylation during seed imbibition, which was enhanced in the *rdo5* mutant. Therefore, RDO5 probably controls seed dormancy by preventing dephosphorylation during seed imbibition. Interestingly, changes in protein levels were relatively minor during imbibition compared to changes in phosphorylation levels.

370 We have previously identified the mRNA binding protein APUM9 to act downstream of RDO5
371 (Xiang et al., 2014). In this work, we identified a general role for APUM9 in seed dormancy that is
372 not restricted to the RDO5 pathway. Factors that enhance dormancy like low seed maturation
373 temperatures and the *DOG6* QTL reduce *APUM9* transcript levels (Figure 6C and 5E). Therefore
374 APUM9 might be a common downstream factor of these dormancy pathways. However, APUM9
375 is probably not part of the DOG1 dormancy pathway because its transcript levels are not affected
376 by DOG1 (Figure 6C). This again confirms regulation of dormancy by independent mechanisms.
377 The first two identified dormancy QTLs, *DOG1* and *RDO5*, are both only expressed in seeds and
378 their mutants exclusively show dormancy and germination defects without pleiotropic phenotypes
379 (Bentsink et al., 2006; Xiang et al., 2014). It is probably no coincidence that these two modifiers of
380 natural variation for seed dormancy are seed-specific. Sequence polymorphisms leading to
381 changes in the expression levels of these genes or their protein function represent an excellent way
382 for plants to adapt their dormancy levels to local environments without simultaneously altering
383 other traits. The properties of *DOG1* and *RDO5* make them highly suitable target genes to
384 manipulate and control seed dormancy levels in crop plants.
385
386 **CONCLUSIONS**
387 Germination timing is an important adaptive trait for plants and is controlled by seed dormancy.
388 Arabidopsis accessions collected in nature show a high variation for dormancy, making it a typical
389 quantitative trait. Finding the genes underlying dormancy quantitative trait loci is a major
390 scientific challenge, which is relevant for agricultural and ecological goals. Here we identified the
391 gene *RDO5* to underlie the dormancy QTL *DOG18*. We show that the RDO5 protein can function
392 as a pseudophosphatase. We found a relatively high number of predicted natural loss-of-function

alleles for *RDO5* that were restricted to northwestern Europe. The loss of RDO5 function could be compensated by low temperatures and by strong alleles of the dormancy QTLs *DOG1*and *DOG6*.

MATERIALS AND METHODS

Plant Materials

NIL DOG6 and NIL DOG18 were a gift from Leónie Bentsink (Wageningen University, the Netherlands). *RDO5* loss-of-function accessions were obtained from the collection of Maarten Koornneef (MPIPZ Cologne, Germany) and originated from the Nottingham Arabidopsis Stock Centre. The *rdo5-1* mutant was described before (Xiang et al., 2014) and has been obtained in a NIL DOG1 background consisting of the L*er* accession with an introgression on chromosome 5, containing the *DOG1* gene from Cvi (Alonso-Blanco et al., 2003). The *rdo5-1* mutant allele in L*er* background was obtained by crossing *rdo5-1* with L*er* and selection against the Cvi introgression fragment in the progeny. Germination tests were performed as described previously (Xiang et al., 2014). Information of primers used in this study can be found in Supplemental Table 4.

DOG18 Map Based Cloning and Complementation Analysis

DOG18 mapping was performed by backcrossing NIL DOG18-Fei-0 with L*er*. Genotyping F2 plants with cleaved-amplified polymorphic sequence markers narrowed the *DOG18* interval into a 700 kb region on chromosome 4, which included the *RDO5* gene. For NIL DOG18-Fei-0 complementation, a genomic fragment, including a 2.7-kb promoter sequence and the *RDO5* coding sequence fused with the HA tag, was amplified from L*er* using gene-specific primers (the HA tag was designed in the reverse primer), cloned into the pDONR207 vector, and transferred into pFASTR01 (Shimada et al., 2010). The binary construct was introduced by

electroporation into *Agrobacterium tumefaciens* strain GV3101, which was subsequently used for transformation by floral dipping (Clough and Bent, 1998). T3 homozygous lines containing single insertion events were used for expression level detection and phenotyping.

Analysis of *DOG18* loss-of- function Natural Variants

The *RDO5* sequence from 855 available accessions was downloaded from Salk *Arabidopsis thaliana* 1001 Genomes. The different types of loss-of-function *RDO5* alleles were confirmed by Sanger sequencing including non-sense mutations (POG-0, HR-10, NFA-8, NFA-10 and Vind-1), Indels (Cam61, Lac-3, An-1, Fei-0 and Durh-1), deletions (Vaar2-6), gene loss (Fr-2), and splicing site mutations (Boot-1). The whole *RDO5* cDNA was sequenced in the accessions of the last four types to confirm the absence of mutations that might restore RDO5 function. For the structure analysis, population structure was inferred using model-based clustering algorithms implemented in the software STRUCTURE, based on 149 genome-wide SNP markers (Lewandowska-Sabat et al., 2010; Platt et al., 2010), using the haploid setting and running 20 replicates with 50,000 and 20,000 MCMC (Markov chain Monte Carlo) iterations of burn-in and after-burning length, respectively (Hubisz et al., 2009). To determine the K number of significantly different genetic clusters, we applied the ΔK method in combination with the absolute value of ln P (X|K) (Evanno et al., 2005) implanted in STRUCTURE HARVESTER (Earl and Vonholdt, 2012). For Haplotype Network analysis, the RDO5 nucleic acid sequence was translated into amino acid sequence according to the standard genetic codes basing on the TAIR 10 ORF. The haplotype network of RDO5 was constructed using Network 4.6 that implements a Reduced Median method (Bandelt et al., 1995).

RNA Extraction, RT-PCR, Protein Extraction and Western Blotting were performed as described previously (Xiang et al., 2014).

3-Dimentional Protein Modeling

A 3D model of full length RDO5 sequence (UniProtKB entry Q9T010 295 amino acids) was constructed using Swiss model software (Arnold et al., 2006). The crystal structure of probable protein phosphatases from rice (UniProtKB entry Q0JLP9 / PDB entry 4oic chain B) was used as template. The model was superimposed on the crystal structure of the complex HAB1/SnRk2,6 (PDB entry: 3ujg chain B) (Soon et al., 2012) using PDBeFold (http://www.ebi.ac.uk/msd-srv/ssm/).

Protein Purification and PP2C Activity Assay

The coding sequences of RDO5 from L*er* and Fei-0, were amplified from cDNA using gene specific primers. The full length of AHG3 was poorly soluble in E.coli, therefore an N terminal deleted AHG3 (ΔNter-N88AHG3) protein was cloned using gene specific primers. N terminal deleted PP2C are reported to be active (Dupeux et al., 2011). RDO5 L*er* and ΔNter-N88AHG3 coding sequence were introduced in pDEST17 expression vector to generate an expression clone with proteins fused with a 6xHis tag in N-terminal. For back mutation (RDO5bm), mutated *RDO5* sequences were synthesized by the Life Technologies Company. To improve solubility of the back-mutated RDO5 protein we generated a construct where RDO5bm is fused with HIS: MBP: TEV in N-terminal. For this purpose, the synthesized sequence was elongated by PCR using gene specific primers to introduce N-terminal fusion TEV cleavage site. Then the PCR product was recombined in pDONR207 and subsequently in pDEST-HIS-MBP (Addagene), constructs were

462 introduced in a BL21-*plyss* strain. Fusion proteins were induced by addition of 0.3mM IPTG in the
463 medium. After overnight culture at 23 °C, cells were harvested by centrifugation and pellets were
464 stored at – 80 °C until purification. Pellets were re-suspended in 50mM HEPES (pH 7.5), 500 mM
465 NaCl, 10 % (v/v) Glycerol, 5 mM DTT, 1 mM PMSF and 25 mM Imidazole, and cells were
466 disrupted by sonication. The soluble fraction was obtained after centrifugation and applied on
467 HisTrap column 1 mL (GE health, USA); the purification process was performed and monitored
468 using ÄKTAprime and Primeview software (GE Health, USA). Elution was performed with the
469 resuspension buffer supplemented with 500mM imidazole. Imidazole was removed from purified
470 protein by gel filtration on PD-10 columns (GE Health, USA) and the protein fraction was
471 concentrated to about 2 $mg.ml^{-1}$ and stored at –80°C. Purified His:MBP:TEV tagged recombinant
472 protein was incubated with HIS:TEV protease and subsequently applied on Ni-NTA agarose
473 (Qiagene, USA) to remove the majority of the His:MBP:TEV tag and HIS:TEV protease. The
474 purity of purified proteins was assessed by SDS-PAGE (Supplemental Figure 7C). Phosphatase
475 activity was measured using the RRA(phosphoT)VA peptide as a substrate. The Serine/Threonine
476 Phosphatase Assay system (Promega, USA) was used for the phosphopeptide assay. Phosphatase
477 assays were performed in 50 µl volumes in half-area, flat-bottom 96 wells plate containing 50 mM
478 Hepes buffer (pH 7.5), 10 mM $MnCl_2$ or $MgCl_2$, 1 mM dithiothreitol (DTT), 0.5µM purified
479 recombinant PP2C proteins and 100 µM peptide substrate. Reaction were performed at 30 °C for
480 30 min and stopped by addition of 50 µL of molybdate dye solution. Absorbance was read at 630
481 mM on a multiscanspektrum (Thermo) 96 well plate reader.
482
483 **Proteolytic Digestion and Desalting**
484 Total protein was extracted in buffer containing 100mM TrisHCl (pH 7.5), 3% SDS, 100mM

DTT, 1X protease inhibitor cocktail, Phosphatase Inhibitor Cocktail 2 and 3 (Sigma,USA). Seed protein extract (2 mg) were processed using the FASP method (Wisniewski et al., 2009) as described in detail in Hartl et al. (2015). Cysteines were alkylated by incubation with 55 mM chloroacetamide in UA buffer (8 M urea, 0.1 M Tris/HCl pH 8.5) for 30 min at room temperature in the dark followed by three washing steps with UA buffer. Incubation with LysC in UA buffer (1:50 enzyme-to-protein ratio) was performed overnight at room temperature. The sample was diluted with ABC buffer (50 mM ammoniumbicarbonate) to a final urea concentration of 2 M urea. Trypsin digestion (1:100 enzyme-to-protein ratio) was performed for 4 h at room temperature. The sample was passed through the filter by centrifugation at 14,000 g for 10 min and residual peptides eluted with 50 µl ABC. Formic acid was added to a final concentration of 0.5% and the sample was desalted using Sep-Pak SPE 1 cc/100 mg (Waters). Solvent was passed through by gravity flow. Columns were conditioned by successive addition of methanol, buffer B (80% acetonitrile (ACN) and 0.5% formic acid (FA)), and buffer A (0.5% FA). The sample was loaded and washed three times with buffer A and eluted twice with buffer B. Eluates were concentrated in a centrifugal evaporator to remove acetonitrile. One tenth of the eluted peptides were processed for whole proteome analysis, the rest was subjected to titanium dioxide enrichment. For total proteome analysis, peptides were desalted and pre-fractionated prior LC-MS/MS into three fractions using the Empore Styrenedivenylbenzene Reversed Phase Sulfonate material (SDB-RPS, 3M) as described in detail by Kulak et al. (2014).

Phosphopeptide Enrichment

Phosphopeptides were enriched with a modified version of the protocol of Melo-Braga et al. (2015). Samples were diluted to 900 µl with 50% ACN, 1% TFA, then 100 µl loading buffer 200

508 mg/ml DHB in 50% ACN, 1% TFA was added. Incubation steps were performed under gentle
509 agitation at room temperature. 6 mg TiO_2 bead (5 mm; GL Science) were suspended in 40 µl
510 loading buffer (20 mg/ml DHB, 50% ACN, 1% TFA) and incubated for 15 min. The first half of
511 the suspension was added to the sample and incubated for 15 min. For removal of liquid, beads
512 were pelleted by centrifugation at 3000 rpm for 1 min. The supernatant was transferred to the
513 second half of the beads suspension and incubated for 15 min. TiO_2 beads from both incubations
514 with bound phosphopeptides were resuspended with loading buffer and combined on C8
515 StageTips (Empore, 3M). Liquid was passed though the tips by centrifugation at 800 g. The beads
516 were washed twice with 80% ACN, 1% TFA and twice with 10% ACN, 0.1% TFA.
517 Phosphopeptides were eluted three times with 5% ammonia and once with 30% ACN by
518 centrifugation at 300 g. Eluates were combined and concentrated in a centrifugal evaporator to
519 remove ammonia. Samples were acidified by adding 1/10 volume of 20% ACN, 10% TFA and
520 desalted with StageTips (Empore C18, 3M) as described as Rappsilber et al. (2007).
521
522 **LC-MS/MS Data Acquisition**
523 Dried peptides were redissolved in 2% ACN, 0.1% TFA for analysis and adjusted to a final
524 concentration of 0.18 µg/µl. Samples were analyzed using an EASY-nLC 1000 (Thermo Fisher)
525 coupled to a Q Exactive Plus mass spectrometer (Thermo Fisher). Peptides were separated on 16
526 cm frit-less silica emitters (New Objective, 0.75 µm inner diameter), packed in-house with
527 reversed-phase ReproSil-Pur C18 AQ 3 µm resin (Dr. Maisch). Peptides (1 µg) were loaded on the
528 column and eluted for 120 min using a segmented linear gradient of 0% to 95% solvent B (solvent
529 A 5% ACN, 0.5% FA; solvent B 100% ACN, 0.5% FA) at a flow-rate of 250 nL/min. Mass spectra
530 were acquired in data-dependent acquisition mode with a TOP15 method. MS spectra were

acquired in the Orbitrap analyzer with a mass range of 300–1750 *m/z* at a resolution of 70,000 FWHM and a target value of $3x10^6$ ions. Precursors were selected with an isolation window of 1.3 *m/z*. HCD fragmentation was performed at a normalized collision energy of 25. MS/MS spectra were acquired with a target value of 10^5 ions at a resolution of 17,500 FWHM and a fixed first mass of *m/z* 100. Peptides with a charge of +1, greater than 6, or with unassigned charge state were excluded from fragmentation for MS2, dynamic exclusion for 30s prevented repeated selection of precursors.

MS Data Analysis

Raw data were processed using MaxQuant software (version 1.5.3.12, http://www.maxquant.org/) with label-free quantification (LFQ) enabled (Cox et al., 2014). MS/MS spectra were searched by the Andromeda search engine against the Arabidopsis TAIR10_pep_20101214 database (ftp://ftp.arabidopsis.org/home/tair/Proteins/TAIR10_protein_lists/). Sequences of 248 common contaminant proteins and decoy sequences were automatically added during the search. Trypsin specificity was required and a maximum of two missed cleavages allowed. Minimal peptide length was set to seven amino acids. Carbamidomethylation of cysteine residues was set as fixed, oxidation of methionine and protein N-terminal acetylation as variable modifications. Phosphorylation of serine, threonine, and tyrosine were added as variable PTMs only for the TiO_2 enriched samples. Peptide-spectrum-matches and proteins were retained if they were below a false discovery rate of 1%. Subsequent quantitative statistical analyses were performed in Perseus (version 1.5.2.6, http://www.maxquant.org/). Identified proteins and phosphorylation sites were processed separately as follows: Hits were only retained if they were quantified in at least two of three replicates in any of the four conditions. LFQ intensities (proteins) and peptide intensities

554 (phosphorylation sites) were log2 transformed. Two-sample t-tests were performed with a *p*-value
555 of 1% as cut-off. Log2 ratios were calculated by replacing missing intensity values with zero.
556
557 **Distribution of Proteins in SeedNet Network**
558 Differently phosphorylated or expressed proteins were submitted to the cytoscape software
559 loading SeedNet network data files, which is publicly available at
560 http://www.vseed.nottingham.ac.uk.
561
562 **Accession Numbers**
563 Sequence data from this article can be found in the Arabidopsis Genome Initiative or
564 GenBank/EMBL databases under the following accession numbers: *RDO5* (At4G11040), *DOG1*
565 (AT5G45830).
566
567 **Supplemental data**
568 The following materials are available in the online version of this article.
569 **Supplemental Figure 1.** Map based cloning of *DOG18*.
570 **Supplemental Figure 2.** *DOG18* Fei-0 allele screening.
571 **Supplemental Figure 3.** *RDO5* transcript level detection in transgenic lines.
572 **Supplemental Figure 4.** Structure estimation of populations for K ranging from one to fourteen
573 by delta K-values.
574 **Supplemental Figure 5.** Germination of *rdo5* segregating populations.
575 **Supplemental Figure 6.** RDO5 sequence analysis.
576 **Supplemental Figure 7.** RDO5 topology structure analysis and SDS PAGE gel of purified

proteins.

Supplemental Figure 8. Localization of differently expressed proteins in the SeedNet network after 6 hours imbibition in wild-type NIL DOG1 (A), *rdo5-1* (B) and potential RDO5 specific targets (C).

Supplemental Table 1. Information of 42 loss-of-function *DOG18* accessions including mutation type, accession name, ID, country, origin, habitat, latitude and longitude of collection site.

Supplemental Table 2. Overview of quantitative mass spectrometry results.

Supplemental Table 3. Overview of regulated phosphosites and phosphorylated protein groups.

Supplemental Table 4. Primers used in this study.

Supplemental Data Set 1. Mass spectrometry results from the phosphoproteome analysis of *rdo5-1* and NIL-DOG1.

ACKNOWLEDGEMENTS

We thank Leónie Bentsink and Maarten Koornneef for providing seed material and Christina Philipp and Anne Harzen for technical assistance. We also thank Carlos Alonso Blanco, William Hughes and Maarten Koornneef for critical reading of the manuscript. This work was supported by the Max Planck Society.

FIGURE LEGENDS

Figure 1. Complementation of *DOG18* by *RDO5*.

(A) Germination after different periods of dry storage of seeds from L*er*, NIL DOG18 and six independent transgenic NIL DOG18 lines containing the *RDO5* gene from L*er*. Shown are means ± SE of six to eight independent batches of seeds for each genotype. (B) Gene structure of *RDO5*

and natural polymorphisms identified in the An-1, Fei-0 and Kas-2 accessions compared to L*er*. Exons are shown as black boxes and introns as lines. (C) Immunoblot analysis of RDO5:HA protein accumulation in seeds of the six NIL DOG18 complementation trangenic lines from (A). Coomassie Brilliant Blue (CBB) staining was used as a loading control.

Figure 2. Complementation of An-1 and Cam61 by *RDO5*.

(A) and (B), Germination after different periods of dry storage of seeds from transgenic lines containing the *RDO5* L*er* allele in An-1 (A) or Cam61 (B) background. Shown are averages ± SE of six to eight independent batches of seeds for each genotype. (C) and (D) qRT-PCR analysis of *APUM9* transcript levels in dry and 6HAI seeds in An-1 (C), Cam61 (D) and their transgenic lines. The expression values were normalized using *ACT8* as control. n = 3 biological replicates; error bars represent SE.

Figure 3. Natural loss-of-function mutations in the *DOG18* gene.

Natural mutations causing predicted *DOG18* loss-of-function alleles are divided into five groups that are shown in separate rows. The location of the mutations for the individual accessions are indicated. Exons (black boxes) are connected with horizontal lines representing intronic regions of *DOG18*. The location of the predicted PP2C domain is indicated at the top.

Figure 4 Geographic distribution, population structure and haplotype network of accessions containing *RDO5* loss-of-function alleles.

(A) Geographical distribution of 42 accessions harboring *RDO5* predicted loss-of-function alleles. (B) Population structure of 95 accessions containing functional or predicted loss-of-function

623 *RDO5* alleles originating from Sweden, UK and Western Europe at K=3. Black stars indicate
624 accessions carrying *RDO5* loss-of-function alleles. (C) *RDO5* haplotype network. Haplotypes are
625 represented by circles with sizes proportional to the number of populations containing that
626 haplotype. Each node represents a single mutation. Black stars indicate accessions or groups
627 carrying *RDO5* loss-of-function alleles.
628
629 **Figure 5 Genetic modifiers of the *RDO5* phenotype.**
630 (A) Dormancy level of 11 accessions with predicted loss-of-function *RDO5* alleles. Col and Cvi
631 are used as low and high dormancy controls. POG-0, HR-10, NFA-8, Vind-1 and NFA-10 belong
632 to the non-sense mutation group, An-1, Fei-0, Lac-3, Cam61 and Durh-1 belong to the indels
633 group, and Fr-2 belongs to the gene loss group. Shown are means ± SE of six to eight independent
634 batches of seeds for each genotype. DSDS50, days of seed dry storage required to reach 50%
635 germination. (B) Immunoblot analysis of DOG1 protein accumulation using a DOG1 antibody in
636 the 11 accessions with predicted loss-of-function *RDO5* alleles. A band from the CBB staining
637 was used as a loading control. The lower panel indicates the DOG1 haplotype of the accessions,
638 ECCY is a strong allele and DSY is a weak allele (Nakabayashi et al., 2015). (C) The correlation of
639 dormancy level and DOG1 protein abundance (quantified from Figure 5B and normalized by the
640 loading control). (D) A strong *DOG6* allele from the Shahdara accession enhances dormancy of
641 the *rdo5-1* mutant (in L*er* background). Germination percentages were determined in freshly
642 harvested seeds. Shown are means ± SE of six to eight independent batches of seeds for each
643 genotype. **P < 0.01 (E) qRT-PCR analysis of *APUM9* transcript levels in L*er, rdo5-1* (L*er*
644 background), NIL DOG6 and *rdo5-1* NIL DOG6 dry and 6HAI seeds. Inset, *APUM9* expression in
645 dry seeds from the different genotypes at a magnified scale. The expression values were

normalized using *ACT8* as control. n = 3 biological replicates; error bars represent SE.

Figure 6. Maternal temperature affects the *RDO5* dormancy phenotype.

(A) Germination of NIL DOG1, *rdo5-1*, *dog1-1* and *rdo5-1 dog1-1* freshly harvested seeds that matured under a day/night regime of 22/16°C or 16/14°C. Shown are means ± SE of six to eight independent batches of seeds for each genotype. (B) qRT-PCR analysis of *RDO5* transcript levels in NIL DOG1 dry and 6HAI seeds that matured under a day/night regime of 22/16°C or 16/14°C. The expression values were normalized using *ACT8* as control. n = 3 biological replicates; error bars represent SE. (C) qRT-PCR analysis of *APUM9* transcript levels in NIL DOG1, *rdo5-1*, *dog1-1* and *rdo5-1 dog1-1* dry and 6HAI seeds that matured under a day/night regime of 22/16°C or 16/14°C. The expression values were normalized using *ACT8* as control. n = 3 biological replicates; error bars represent SE.

Figure 7. RDO5 functions as a pseudophosphatase.

(A) Phosphatase activity is restored in RDO5 after backmutations. Phosphatase activity of RDO5 and RDO5 back-mutation (RDO5bm) proteins was measured *in vitro* using the RRA(phosphoT)VA peptide as a substrate. ΔC-terN88AHG3 was used as a positive control. Data are averages ± SE from three replicates. (B) Venn diagram analyses showing common and differential distribution of phosphorylated sites identified in NIL DOG1 and *rdo5-1* after six hours imbibition compared with dry seeds. (C)-(E) Localization in the SeedNet network of differentially phosphorylated proteins from wild-type NIL DOG1 (C), *rdo5-1* (D) and differentially phosphorylated proteins present in *rdo5-1* but not in NIL DOG1 (E) after six hours imbibition compared with dry seeds. The regions outlined in green correspond to clusters associated with

669 dormancy (region 1) or germination (regions 2 and 3). The red dots represent proteins with
670 decreased phosphorylation levels and the blue dots represent proteins with increased
671 phosphorylation levels.
672
673

Parsed Citations

Alonso-Blanco, C., Bentsink, L., Hanhart, C.J., Blankestijn-de Vries, H., and Koornneef, M. (2003). Analysis of natural allelic variation at seed dormancy loci of Arabidopsis thaliana. Genetics 164, 711-729.

Pubmed: Author and Title
CrossRef: Author and Title
Google Scholar: Author Only Title Only Author and Title

Amiguet-Vercher, A., Santuari, L., Gonzalez-Guzman, M., Depuydt, S., Rodriguez, P.L., and Hardtke, C.S. (2015). The IBO germination quantitative trait locus encodes a phosphatase 2C-related variant with a nonsynonymous amino acid change that interferes with abscisic acid signaling. New Phytol. 205, 1076-1082.

Pubmed: Author and Title
CrossRef: Author and Title
Google Scholar: Author Only Title Only Author and Title

Arnold, K., Bordoli, L., Kopp, J., and Schwede, T. (2006). The SWISS-MODEL workspace: a web-based environment for protein structure homology modelling. Bioinformatics 22, 195-201.

Pubmed: Author and Title
CrossRef: Author and Title
Google Scholar: Author Only Title Only Author and Title

Ashikawa, I., Abe, F., and Nakamura, S. (2010). Ectopic expression of wheat and barley DOG1-like genes promotes seed dormancy in Arabidopsis. Plant Sci. 179, 536-542.

Pubmed: Author and Title
CrossRef: Author and Title
Google Scholar: Author Only Title Only Author and Title

Bandelt, H.J., Forster, P., Sykes, B.C., and Richards, M.B. (1995). Mitochondrial Portraits of Human-Populations Using Median Networks. Genetics 141, 743-753.

Pubmed: Author and Title
CrossRef: Author and Title
Google Scholar: Author Only Title Only Author and Title

Bassel, G.W., Lan, H., Glaab, E., Gibbs, D.J., Gerjets, T., Krasnogor, N., Bonner, A.J., Holdsworth, M.J., and Provart, N.J. (2011). Genome-wide network model capturing seed germination reveals coordinated regulation of plant cellular phase transitions. Proc. Natl. Acad. Sci. USA 108, 9709-9714.

Pubmed: Author and Title
CrossRef: Author and Title
Google Scholar: Author Only Title Only Author and Title

Bentsink, L., Jowett, J., Hanhart, C.J., and Koornneef, M. (2006). Cloning of DOG1, a quantitative trait locus controlling seed dormancy in Arabidopsis. Proc. Natl. Acad. Sci. USA 103, 17042-17047.

Pubmed: Author and Title
CrossRef: Author and Title
Google Scholar: Author Only Title Only Author and Title

Bentsink, L., Hanson, J., Hanhart, C.J., Blankestijn-de Vries, H., Coltrane, C., Keizer, P., El-Lithy, M., Alonso-Blanco, C., de Andres, M.T., Reymond, M., van Eeuwijk, F., Smeekens, S., and Koornneef, M. (2010). Natural variation for seed dormancy in Arabidopsis is regulated by additive genetic and molecular pathways. Proc. Natl. Acad. Sci. USA 107, 4264-4269.

Pubmed: Author and Title
CrossRef: Author and Title
Google Scholar: Author Only Title Only Author and Title

Clough, S.J., and Bent, A.F. (1998). Floral dip: a simplified method for Agrobacterium-mediated transformation of Arabidopsis thaliana. Plant J. 16, 735-743.

Pubmed: Author and Title
CrossRef: Author and Title
Google Scholar: Author Only Title Only Author and Title

Conner, S.H., Kular, G., Peggie, M., Shepherd, S., Schuttelkopf, A.W., Cohen, P., and Van Aalten, D.M.F. (2006). TAK1-binding protein 1 is a pseudophosphatase. Biochem J. 399, 427-434.

Pubmed: Author and Title
CrossRef: Author and Title
Google Scholar: Author Only Title Only Author and Title

Cox, J., Hein, M.Y., Luber, C.A., Paron, I., Nagaraj, N., and Mann, M. (2014). Accurate proteome-wide label-free quantification by delayed normalization and maximal peptide ratio extraction, termed MaxLFQ. Molecular & cellular proteomics 13, 2513-2526.

Pubmed: Author and Title
CrossRef: Author and Title
Google Scholar: Author Only Title Only Author and Title

Dupeux, F., Antoni, R., Betz, K., Santiago, J., Gonzalez-Guzman, M., Rodriguez, L., Rubio, S., Park, S.Y., Cutler, S.R., Rodriguez, P.L., and Marquez, J.A. (2011). Modulation of Abscisic Acid Signaling in Vivo by an Engineered Receptor-Insensitive Protein Phosphatase Type 2C Allele. Plant Physiol. 156, 106-116.

Pubmed: Author and Title
CrossRef: Author and Title
Google Scholar: Author Only Title Only Author and Title

Earl, D.A., and Vonholdt, B.M. (2012). STRUCTURE HARVESTER: a website and program for visualizing STRUCTURE output and

implementing the Evanno method. Conserv. Genet. Resour. 4, 359-361.
Pubmed: Author and Title
CrossRef: Author and Title
Google Scholar: Author Only Title Only Author and Title

Evanno, G., Regnaut, S., and Goudet, J. (2005). Detecting the number of clusters of individuals using the software STRUCTURE: a simulation study. Mol. Ecol. 14, 2611-2620.
Pubmed: Author and Title
CrossRef: Author and Title
Google Scholar: Author Only Title Only Author and Title

Footitt, S., Douterelo-Soler, I., Clay, H., and Finch-Savage, W.E. (2011). Dormancy cycling in Arabidopsis seeds is controlled by seasonally distinct hormone-signaling pathways. Proc. Natl. Acad. Sci. USA 108, 20236-20241.
Pubmed: Author and Title
CrossRef: Author and Title
Google Scholar: Author Only Title Only Author and Title

Gosti, F., Beaudoin, N., Serizet, C., Webb, A.A., Vartanian, N., and Giraudat, J. (1999). ABI1 protein phosphatase 2C is a negative regulator of abscisic acid signaling. Plant Cell 11, 1897-1910.
Pubmed: Author and Title
CrossRef: Author and Title
Google Scholar: Author Only Title Only Author and Title

Graeber, K., Nakabayashi, K., Miatton, E., Leubner-Metzger, G., and Soppe, W.J.J. (2012). Molecular mechanisms of seed dormancy. Plant Cell Environ. 35, 1769-1786.
Pubmed: Author and Title
CrossRef: Author and Title
Google Scholar: Author Only Title Only Author and Title

Graeber, K., Linkies, A., Muller, K., Wunchova, A., Rott, A., and Leubner-Metzger, G. (2010). Cross-species approaches to seed dormancy and germination: conservation and biodiversity of ABA-regulated mechanisms and the Brassicaceae DOG1 genes. Plant Mol. Biol 73, 67-87.
Pubmed: Author and Title
CrossRef: Author and Title
Google Scholar: Author Only Title Only Author and Title

Hartl., M., König., A.-C., and Finkemeier., I. (2015). Identification of Lysine-Acetylated Mitochondrial Proteins and Their Acetylation Sites. Methods in Molecular Biology 1305, 107-121.
Pubmed: Author and Title
CrossRef: Author and Title
Google Scholar: Author Only Title Only Author and Title

He, H.Z., Vidigal, D.D., Snoek, L.B., Schnabel, S., Nijveen, H., Hilhorst, H., and Bentsink, L. (2014). Interaction between parental environment and genotype affects plant and seed performance in Arabidopsis. J Exp. Bot. 65, 6603-6615.
Pubmed: Author and Title
CrossRef: Author and Title
Google Scholar: Author Only Title Only Author and Title

Hubisz, M.J., Falush, D., Stephens, M., and Pritchard, J.K. (2009). Inferring weak population structure with the assistance of sample group information. Mol. Ecol. Resour. 9, 1322-1332.
Pubmed: Author and Title
CrossRef: Author and Title
Google Scholar: Author Only Title Only Author and Title

Kendall, S.L., Hellwege, A., Marriot, P., Whalley, C., Graham, I.A., and Penfield, S. (2011). Induction of Dormancy in Arabidopsis Summer Annuals Requires Parallel Regulation of DOG1 and Hormone Metabolism by Low Temperature and CBF Transcription Factors. Plant Cell 23, 2568-2580.
Pubmed: Author and Title
CrossRef: Author and Title
Google Scholar: Author Only Title Only Author and Title

Kim, W., Lee, Y., Park, J., Lee, N., and Choi, G. (2013). HONSU, a protein phosphatase 2C, regulates seed dormancy by inhibiting ABA signaling in Arabidopsis. Plant Cell Physiol. 54, 555-572.
Pubmed: Author and Title
CrossRef: Author and Title
Google Scholar: Author Only Title Only Author and Title

Kulak, N.A., Pichler, G., Paron, I., Nagaraj, N., and Mann, M. (2014). Minimal, encapsulated proteomic-sample processing applied to copy-number estimation in eukaryotic cells. Nat. Methods 11, 319-324.
Pubmed: Author and Title
CrossRef: Author and Title
Google Scholar: Author Only Title Only Author and Title

Lewandowska-Sabat, A.M., Fjellheim, S., and Rognli, O.A. (2010). Extremely low genetic variability and highly structured local populations of Arabidopsis thaliana at higher latitudes. Mol. Ecol. 19, 4753-4764.
Pubmed: Author and Title
CrossRef: Author and Title
Google Scholar: Author Only Title Only Author and Title

Li, Y., Huang, Y., Bergelson, J., Nordborg, M., and Borevitz, J.O. (2010). Association mapping of local climate-sensitive quantitative

trait loci in Arabidopsis thaliana. Proc. Natl. Acad. Sci. USA 107, 21199-21204.
Pubmed: Author and Title
CrossRef: Author and Title
Google Scholar: Author Only Title Only Author and Title

Melo-Braga, M.N., Ibanez-Vea, M., Larsen, M.R., and Kulej, K. (2015). Comprehensive protocol to simultaneously study protein phosphorylation, acetylation, and N-linked sialylated glycosylation. Methods in molecular biology 1295, 275-292.
Pubmed: Author and Title
CrossRef: Author and Title
Google Scholar: Author Only Title Only Author and Title

Nakabayashi, K., Bartsch, M., Ding, J., and Soppe, W.J.J. (2015). Seed Dormancy in Arabidopsis Requires Self-Binding Ability of DOG1 Protein and the Presence of Multiple Isoforms Generated by Alternative Splicing. Plos Genet. 11, e1005737.
Pubmed: Author and Title
CrossRef: Author and Title
Google Scholar: Author Only Title Only Author and Title

Nakabayashi, K., Bartsch, M., Xiang, Y., Miatton, E., Pellengahr, S., Yano, R., Seo, M., and Soppe, W.J.J. (2012). The Time Required for Dormancy Release in Arabidopsis Is Determined by DELAY OF GERMINATION1 Protein Levels in Freshly Harvested Seeds. Plant Cell 24, 2826-2838.
Pubmed: Author and Title
CrossRef: Author and Title
Google Scholar: Author Only Title Only Author and Title

Nambara, E., Okamoto, M., Tatematsu, K., Yano, R., Seo, M., and Kamiya, Y. (2010). Abscisic acid and the control of seed dormancy and germination. Seed Sci. Res. 20, 55-67.
Pubmed: Author and Title
CrossRef: Author and Title
Google Scholar: Author Only Title Only Author and Title

Nishimura, N., Yoshida, T., Kitahata, N., Asami, T., Shinozaki, K., and Hirayama, T. (2007). ABA-Hypersensitive Germination1 encodes a protein phosphatase 2C, an essential component of abscisic acid signaling in Arabidopsis seed. Plant J. 50, 935-949.
Pubmed: Author and Title
CrossRef: Author and Title
Google Scholar: Author Only Title Only Author and Title

Park, S.Y., Fung, P., Nishimura, N., Jensen, D.R., Fujii, H., Zhao, Y., Lumba, S., Santiago, J., Rodrigues, A., Chow, T.F., Alfred, S.E., Bonetta, D., Finkelstein, R., Provart, N.J., Desveaux, D., Rodriguez, P.L., McCourt, P., Zhu, J.K., Schroeder, J.I., Volkman, B.F., and Cutler, S.R. (2009). Abscisic acid inhibits type 2C protein phosphatases via the PYR/PYL family of START proteins. Science 324, 1068-1071.
Pubmed: Author and Title
CrossRef: Author and Title
Google Scholar: Author Only Title Only Author and Title

Platt, A., Horton, M., Huang, Y.S., Li, Y., Anastasio, A.E., Mulyati, N.W., Agren, J., Bossdorf, O., Byers, D., Donohue, K., Dunning, M., Holub, E.B., Hudson, A., Le Corre, V., Loudet, O., Roux, F., Warthmann, N., Weigel, D., Rivero, L., Scholl, R., Nordborg, M., Bergelson, J., and Borevitz, J.O. (2010). The scale of population structure in Arabidopsis thaliana. Plos Genet. 6, e1000843.
Pubmed: Author and Title
CrossRef: Author and Title
Google Scholar: Author Only Title Only Author and Title

Postma, F.M., and Agren, J. (2015). Maternal environment affects the genetic basis of seed dormancy in Arabidopsis thaliana. Mol. Ecol. 24, 785-797.
Pubmed: Author and Title
CrossRef: Author and Title
Google Scholar: Author Only Title Only Author and Title

Rappsilber, J., Mann, M., and Ishihama, Y. (2007). Protocol for micro-purification, enrichment, pre-fractionation and storage of peptides for proteomics using StageTips. Nat. Protoc. 2, 1896-1906.
Pubmed: Author and Title
CrossRef: Author and Title
Google Scholar: Author Only Title Only Author and Title

Reiterer, V., Eyers, P.A., and Farhan, H. (2014). Day of the dead: pseudokinases and pseudophosphatases in physiology and disease. Trends Cell Biol. 24, 489-505.
Pubmed: Author and Title
CrossRef: Author and Title
Google Scholar: Author Only Title Only Author and Title

Robert, N., Merlot, S., N'Guyen, V., Boisson-Dernier, A., and Schroeder, J.I. (2006). A hypermorphic mutation in the protein phosphatase 2C HAB1 strongly affects ABA signaling in Arabidopsis. FEBS Lett. 580, 4691-4696.
Pubmed: Author and Title
CrossRef: Author and Title
Google Scholar: Author Only Title Only Author and Title

Rodriguez, P.L., Benning, G., and Grill, E. (1998). ABI2, a second protein phosphatase 2C involved in abscisic acid signal transduction in Arabidopsis. FEBS Lett. 421, 185-190.
Pubmed: Author and Title
CrossRef: Author and Title
Google Scholar: Author Only Title Only Author and Title

Shimada, T.L., Shimada, T., and Hara-Nishimura, I. (2010). A rapid and non-destructive screenable marker, FAST, for identifying transformed seeds of Arabidopsis thaliana. Plant J. 61, 519-528.
Pubmed: Author and Title
CrossRef: Author and Title
Google Scholar: Author Only Title Only Author and Title

Soon, F.F., Ng, L.M., Zhou, X.E., West, G.M., Kovach, A., Tan, M.H., Suino-Powell, K.M., He, Y., Xu, Y., Chalmers, M.J., Brunzelle, J.S., Zhang, H., Yang, H., Jiang, H., Li, J., Yong, E.L., Cutler, S., Zhu, J.K., Griffin, P.R., Melcher, K., and Xu, H.E. (2012). Molecular mimicry regulates ABA signaling by SnRK2 kinases and PP2C phosphatases. Science 335, 85-88.
Pubmed: Author and Title
CrossRef: Author and Title
Google Scholar: Author Only Title Only Author and Title

Springthorpe, V., and Penfield, S. (2015). Flowering time and seed dormancy control use external coincidence to generate life history strategy. eLife 4.
Pubmed: Author and Title
CrossRef: Author and Title
Google Scholar: Author Only Title Only Author and Title

Wisniewski, J.R., Zougman, A., and Mann, M. (2009). Combination of FASP and StageTip-based fractionation allows in-depth analysis of the hippocampal membrane proteome. J Proteome Res. 8, 5674-5678.
Pubmed: Author and Title
CrossRef: Author and Title
Google Scholar: Author Only Title Only Author and Title

Xiang, Y., Nakabayashi, K., Ding, J., He, F., Bentsink, L., and Soppe, W.J.J. (2014). REDUCED DORMANCY5 Encodes a Protein Phosphatase 2C That Is Required for Seed Dormancy in Arabidopsis. Plant Cell 26, 4362-4375.
Pubmed: Author and Title
CrossRef: Author and Title
Google Scholar: Author Only Title Only Author and Title

Yoshida, T., Nishimura, N., Kitahata, N., Kuromori, T., Ito, T., Asami, T., Shinozaki, K., and Hirayama, T. (2006). ABA-hypersensitive germination 3 encodes a protein phosphatase 2C (AtPP2CA) that strongly regulates abscisic acid signaling during germination among Arabidopsis protein phosphatase 2Cs. Plant Physiol. 140, 115-126.
Pubmed: Author and Title
CrossRef: Author and Title
Google Scholar: Author Only Title Only Author and Title